Sodium Metal Anode with Multiphasic Interphase for Room Temperature Sodium-Sulfur Pouch Cells

Chhail Bihari Soni[1], Sidhant Kumar Barik[4], Vineeth S.K.[1,3], Bhupendra Yadav,[1,2], Mahesh Chandra[1], Sungjemmenla[1], Sanjay Kumar[1], Hemant Kumar[4], and Vipin Kumar[1,2]*

[1]Department of Energy Science and Engineering, Indian Institute of Technology Delhi, Hauz Khas, New Delhi, 110016, India

[2]Department of Physics, Indian Institute of Technology Delhi, Hauz Khas, New Delhi, 110016, India

[3]University of Queensland–IIT Delhi Academy of Research (UQIDAR), Indian Institute of Technology Delhi, Hauz Khas, New Delhi 110016, India

[4]School of Basic Sciences, Indian Institute of Technology Bhubaneswar, Odisha, 752050, India

*Email id: vkumar@dese.iitd.ac.in

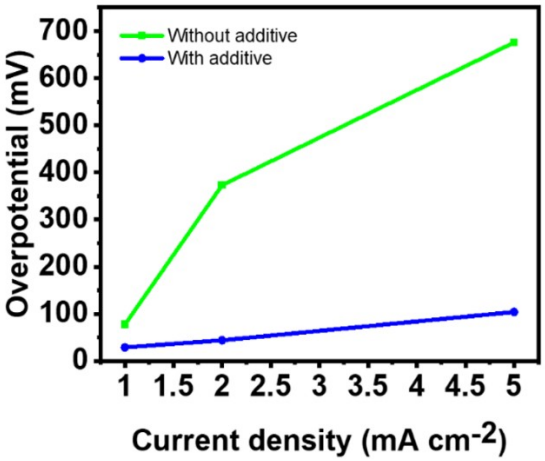

Figure-S1 Sodium symmetric cell (Na//Na) overpotential as a function of current density

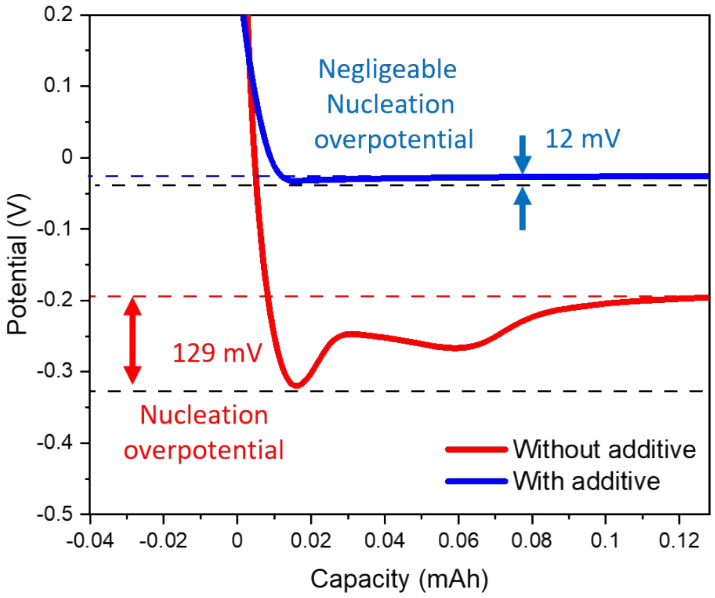

Figure-S2 Nucleation overpotential of Na//Cu half-cell with additive and without additive at 1 mA cm^{-2} current density and 1 mAh cm^{-2} specific capacity.

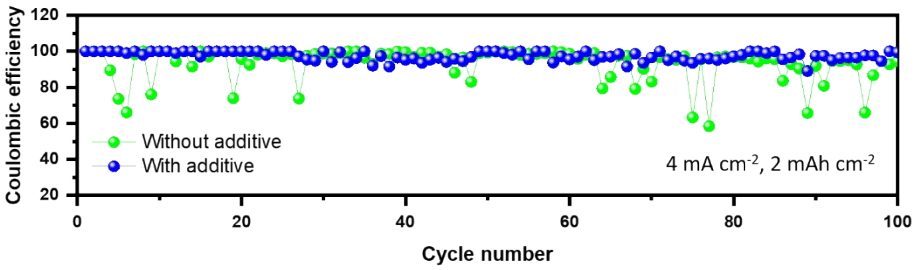

Figure-S3 Coulombic efficiency of Na//Cu half cells at a current density of 4 mA cm^{-2} and capacity of 2 mA h cm^{-2}

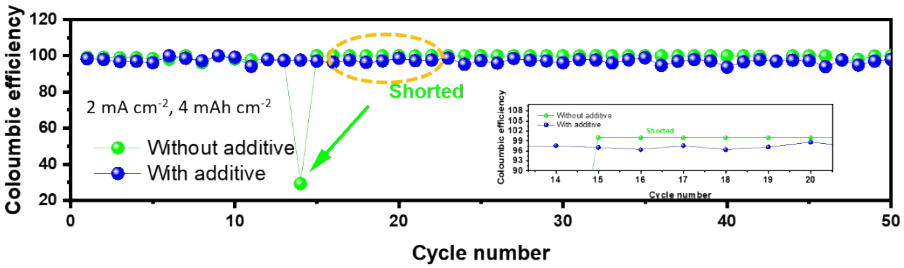

Figure-S4 Coulombic efficiency of Na//Cu half cells at a current density of 2 mA cm^{-2} and capacity of 4 mA h cm^{-2} specific capacity

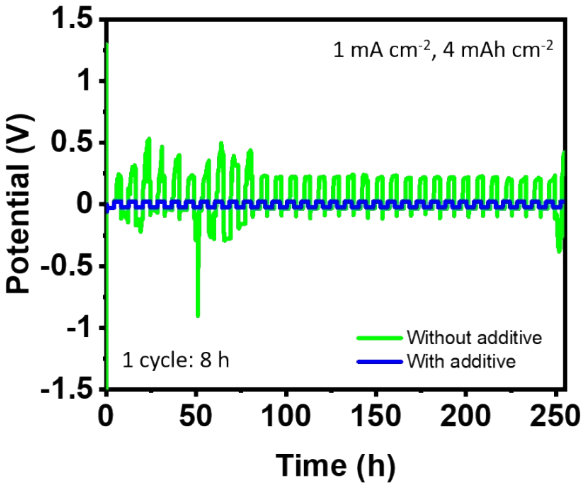

Figure-S5 Na//Na symmetric cell plating/stripping profile with additive and without additive at 1 mA cm^{-2} current density and 4 mA h cm^{-2} specific capacity.

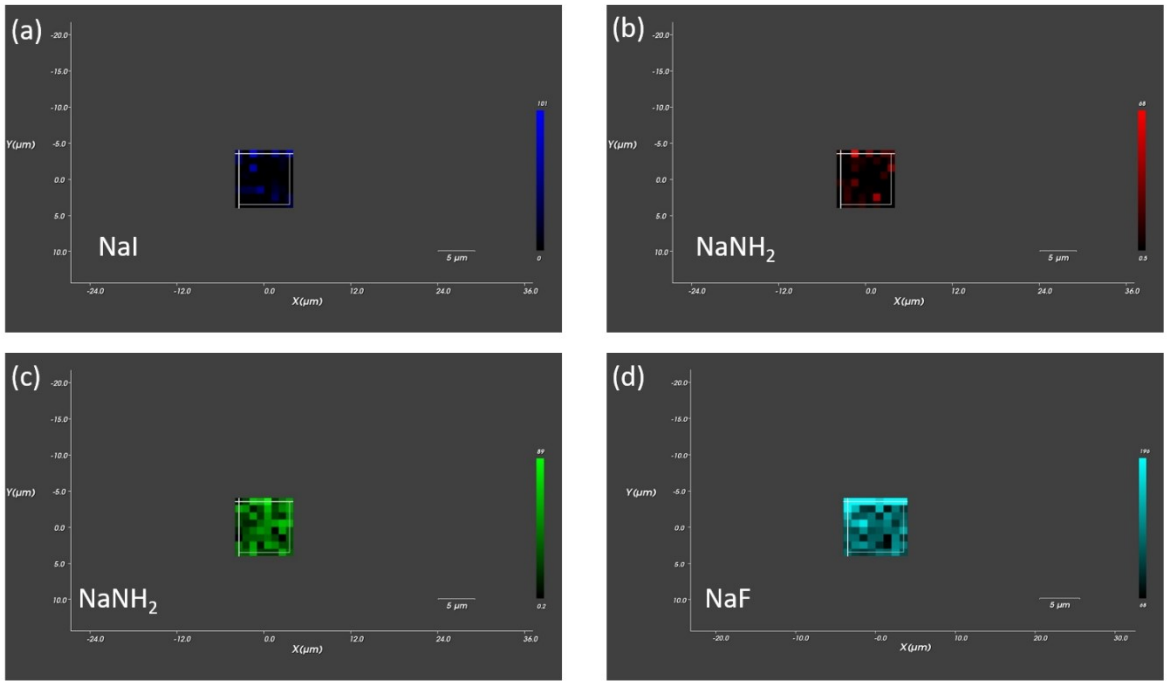

Figure-S6 Raman mapping of different SEI species present on the surface of sodium metal anode after cycling (a) NaI distribution throughout the multiple scans in a region of 5 µm x 5 µm around 185 cm^{-1} Raman shift (b) $NaNH_2$ distribution throughout the multiple scans in a region of 5 µm x 5 µm around 225 cm^{-1} Raman shift (c) $NaNH_2$ distribution throughout the multiple scans in a region of 5 µm x 5 µm around 344 cm^{-1} Raman shift (d) NaF distribution throughout the multiple scans in a region of 5 µm x 5 µm around 511 cm^{-1} Raman shift

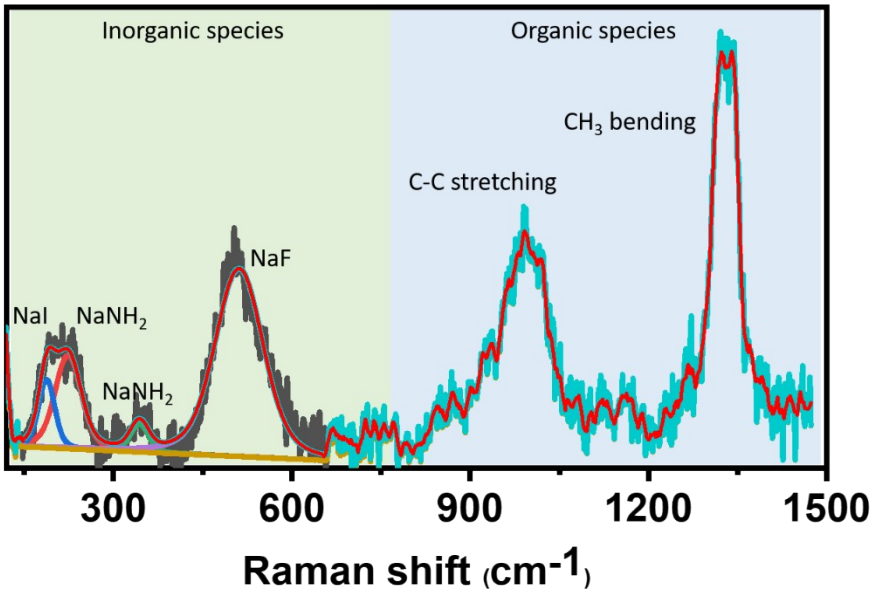

Figure-S7 Raman spectrum of sodium metal anode after 20 plating/stripping cycles in a symmetric cell configuration showing organic and inorganic components in the SEI

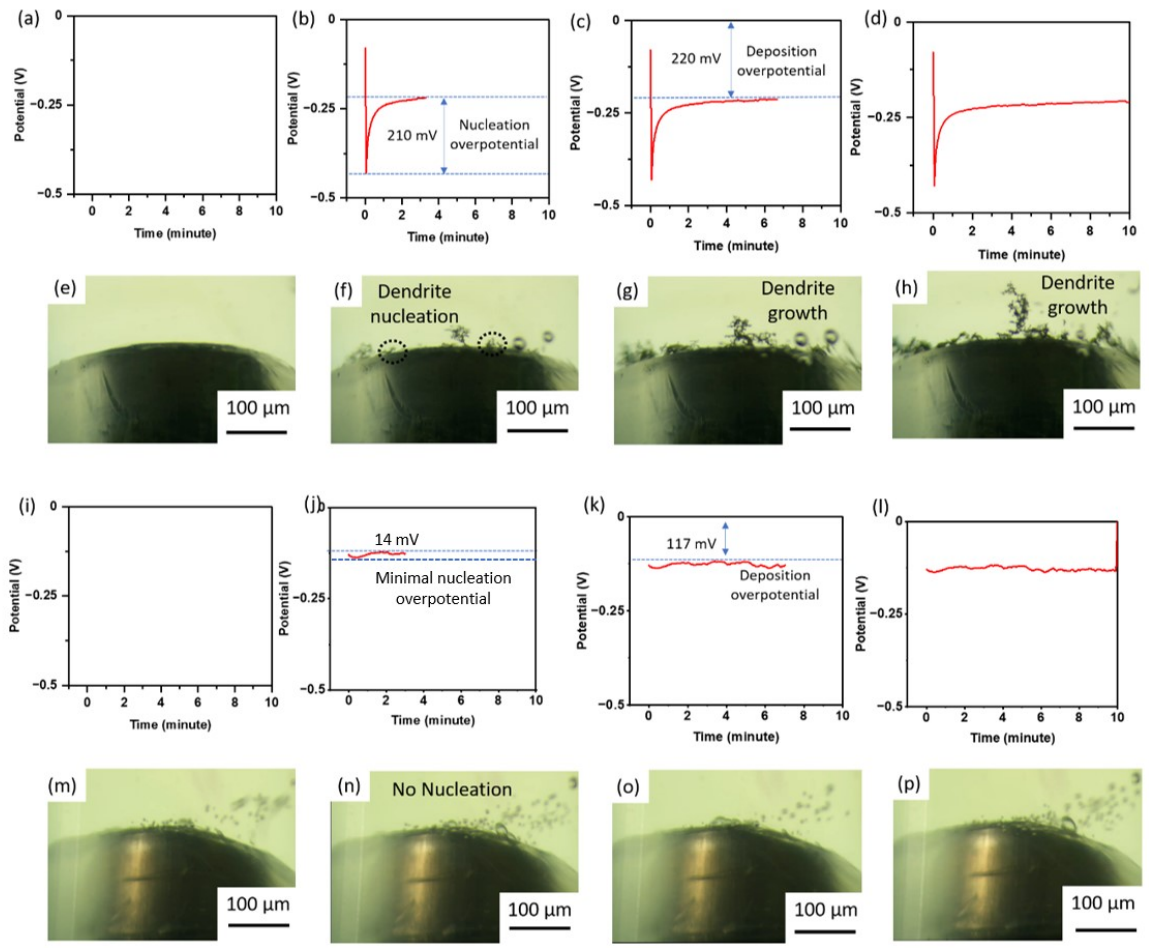

Figure-S8 *In-situ* optical cell testing of sodium metal anode in both the electrolyte systems. (a and e, without additive) at the starting stage of deposition (b and f) after nucleation from 0 to 3 minute of deposition (c and g) nucleation to growth region (d and h) sodium dendrite growth region up to 10 min. (i-m, with additive) at the starting stage of deposition (j and n) after nucleation from 0 to 3 minute of deposition, very less nucleation overpotential (k and o) deposition region (l and p) deposition region up to 10 min.

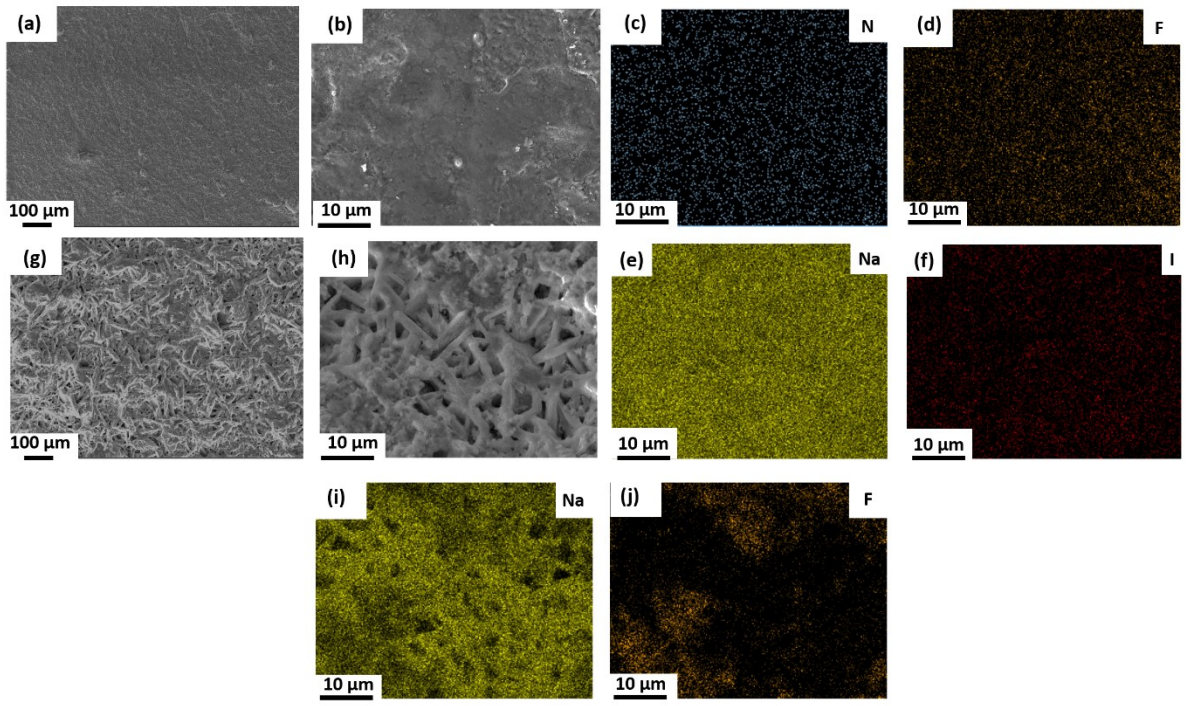

Figure-S9 FESEM images of the sodium surface after 20 plating/stripping cycles in a Na//Na symmetric cell at 1 mA cm^{-2} current density. (a, b) Na surface cycled in MI based electrolyte (c-f) corresponding EDX mapping of sodium anode comprising N, F, Na and I in the deposited layer. (g, h) Na surface in the reference electrolyte cell (i, j) EDX mapping of sodium anode comprising Na and F in the deposited layer.

Table-S1 A fair comparison of Na//Na symmetric cell performance parameters i.e., overpotential and cycle number

Cell type	Salt	Solvent	Additive	Current density (mA cm^{-2})	Capacity (mA h cm^{-2})	Overpotential (m V)	Cycle life (h)
Na//Na (This work)	**1 M NaOTf**	**Diglyme**	**100 mM Methylammonium iodide**	**1**	**1**	**30-35**	**>3200**
Na//Na[1]	0.8 M NaPF6	TMP/ FEC	DTD as co-solvent	0.5	1	200	1350

		(7:3)					
Na//Na[2]	1 M $NaPF_6$	EC/PC	2% TMDT	0.5	1	400	450
Na//Na[3]	0.3 M $NaPF_6$	EC/PC	Acetamide (BSTFA)	0.5	0.5	120	350
Na//Na[4]	4 M NaFSI	DMC	1% SbF_3	0.5	0.5	25	1000
Na//Na[5]	1 M NaTFSI	FEC	0.75 % $NaAsF_6$	0.5	1	500	350
Na//Na[6]	2 M $NaPF_6$	DME/ FEPE	1% SbF_3	0.5	0.5	200	1200
Na//Na[7]	1 M $NaClO_4$	EC/DEC	0.05 M $SnCl_2$	0.5	1	100	500
Na//Na[8]	1 M $NaPF_6$	Diglyme	0.033 M Na_2S_6	2	1	38	400
Na//Na[9]	1 M $NaPF_6$	EC/PC	FEC	1	1	100	100
Na//Na[10]	1 M NaOTf	Diglyme	100 mM 9-Fluorenone	1	1	30	1200
Na//Na[11]	1 M $NaPF_6$	EC/PC	1 Wt% Perfluorobenzene	1	1	80	600
Na//Na[12]	1 M $NaPF_6$	Diglyme	Cetyltrimethylammonium bromide	3	3	500	80

Table-S2 Resistance value from EIS data after fitting for both the electrolyte system at different temperature

S. No.	Temperature	Cell	Resistance (R)
1	10 °C (283K)	With additive Without additive	103.56 241.82

2	20 °C (293K)	With additive Without additive	60.43 134.61
3	30 °C (303K)	With additive Without additive	44.30 115.33
4	40 °C (313K)	With additive Without additive	29.87 90.47
6	50 °C (323K)	With additive Without additive	26.88 61.20
6	60 °C (333K)	With additive Without additive	20.14 47.63

Table-S3 XPS peak assignments for organic species in SEI with additive

Element	Peak position	Peak assignment	Species
C	288.2/286.5/284.8 eV	C-O/ /C=O /C-C, C-H	RCH_2ONa
O	531/535.5	Na-O, C=O/C-O	RCH_2ONa, Na_2O

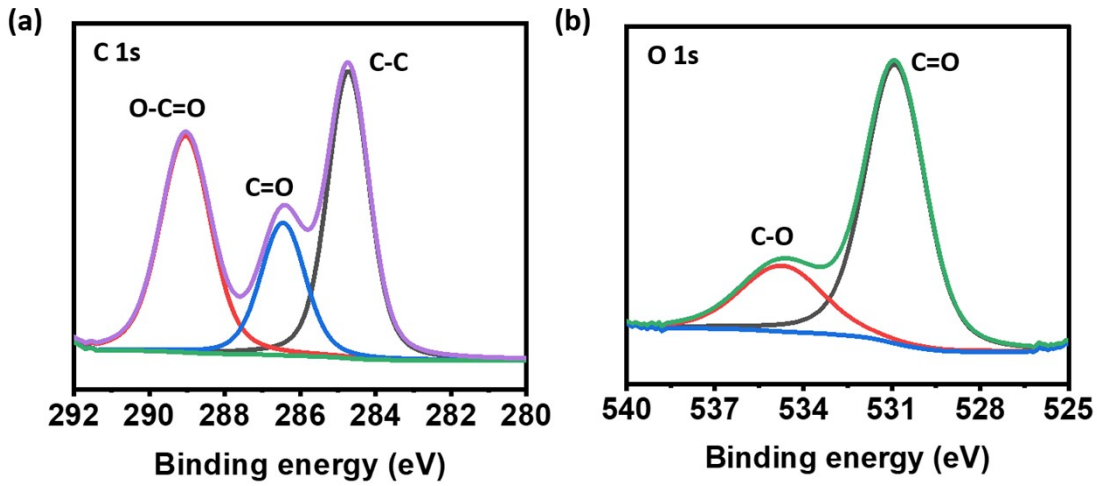

Figure-S10 High-resolution XPS spectra of Na metal anode after 20 plating/stripping cycles at 1 mA cm^{-2} current density for (a) C1s and (b) O1s showing organic components in the SEI

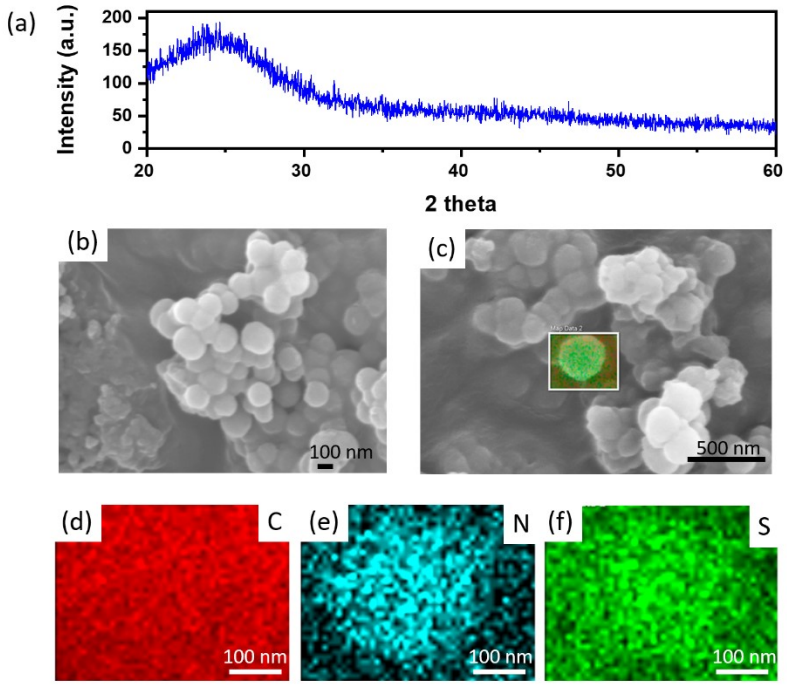

Figure-S11 Microscopic and elemental analysis of the as-synthesized SPAN cathode material (a) showing XRD spectra for said material, all the peaks are corresponding to SPAN (b-c) FESEM images of SPAN powder (d-f) EDX analysis of the said material showing the uniform distribution of N and S in the material

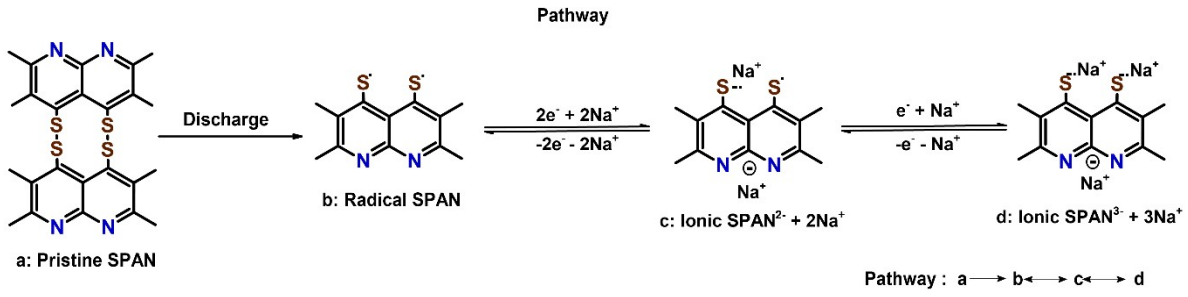

Figure-S12 The possible reaction pathways of SPAN cathode[13]

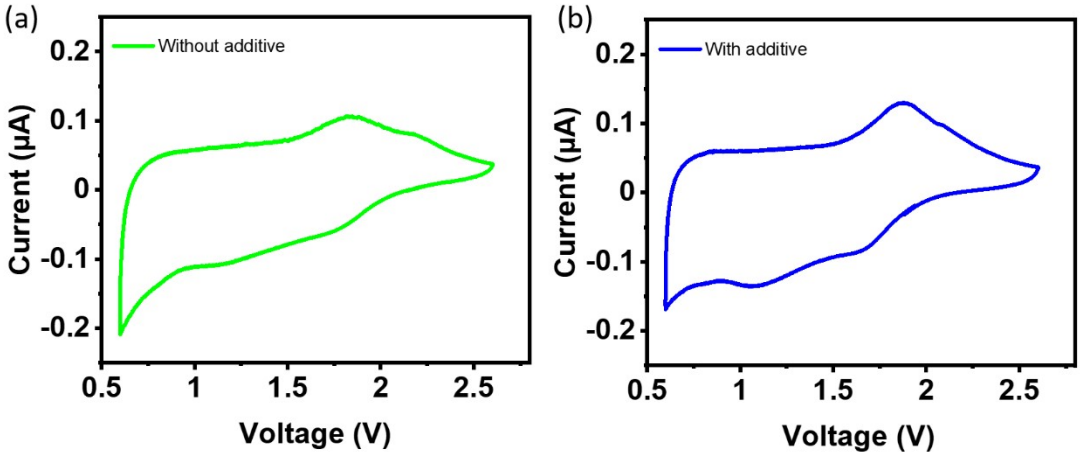

Figure-S13 Cyclic voltammogram for Na//SPAN full cells (a) without and (b) with additive. CVs were conducted at a scan rate of 0.1 mV s^{-1} in a potential window of 0.6 to 2.6 V

References

1 M. Zhu, L. Li, Y. Zhang, K. Wu, F. Yu, Z. Huang, G. Wang, J. Li, L. Wen, H. K. Liu, S. X. Dou, Y. Yu and C. Wu, *Energy Storage Mater.*, 2021, **42**, 145–153.

2 M. Zhu, Y. Zhang, F. Yu, Z. Huang, Y. Zhang, L. Li, G. Wang, L. Wen, H. K. Liu, S. X. Dou and C. Wu, *Nano Lett.*, 2021, **21**, 619–627.

3 R. Jiang, L. Hong, Y. Liu, Y. Wang, S. Patel, X. Feng and H. Xiang, *Energy Storage Mater.*, 2021, **42**, 370–379.

4 W. Fang, H. Jiang, Y. Zheng, H. Zheng, X. Liang, Y. Sun, C. Chen and H. Xiang, *J. Power Sources*, 2020, **455**, 227956.

5 S. Wang, W. Cai, Z. Sun, F. Huang, Y. Jie, Y. Liu, Y. Chen, B. Peng, R. Cao, G. Zhang and S. Jiao, *Chem. Commun.*, 2019, **55**, 14375–14378.

6 W. Fang, R. Jiang, H. Zheng, Y. Zheng, Y. Sun, X. Liang, H. F. Xiang, Y. Z. Feng and Y. Yu, *Rare Met.*, 2021, **40**, 433–439.

7 X. Zheng, H. Fu, C. Hu, H. Xu, Y. Huang, J. Wen, H. Sun, W. Luo and Y. Huang, *J. Phys. Chem. Lett.*, 2019, **10**, 707–714.

8 H. Wang, C. Wang, E. Matios and W. Li, *Angew. Chemie*, 2018, **130**, 7860–7863.

9 M. Han, C. Zhu, T. Ma, Z. Pan, Z. Tao and J. Chen, *Chem. Commun.*, 2018, **54**, 2381–2384.

10 C. Bihari, S. Bera, S. K. Vineeth, H. Kumar and V. Kumar, *J. Energy Storage*, 2023, **71**, 108132.

11 C. Zhu, D. Wu, Z. Wang, H. Wang, J. Liu, K. Guo, Q. Liu and J. Ma, *Adv. Funct. Mater.*, 2024, **34**, 1–9.

12 J. Luo, Y. Zhang, E. Matios, P. Wang, C. Wang, Y. Xu, X. Hu, H. Wang, B. Li and W. Li, *Nano Lett.*, 2022, **22**, 1382–1390.

13 C. Sanjaykumar, N. Sungjemmenla, M. Chandra, C. B. Soni, S. K. Vineeth, S. Das, N. Cohen, H. Kumar, D. Mandler and V. Kumar, *J. Mater. Chem. A*, 2024, 1420–1429.